Journal of Organometallic Chemistry, 256 (1983) 375–389
Elsevier Sequoia S.A., Lausanne – Printed in The Netherlands

PHOSPHORUS COORDINATION OF DI- AND TRI-AZAPHOSPHOLES IN PLATINUM(0) COMPLEXES: X-RAY MOLECULAR STRUCTURE OF TRIS(TRIPHENYLPHOSPHINE)-1,5-DIMETHYL-1,2,4,3-TRIAZAPHOSPHOLE PLATINUM(0) [$Pt(PPh_3)_3\overline{P{=}NN(Me)C(Me){=}N}$]

JOHANNA G. KRAAIJKAMP, GERARD VAN KOTEN *, KEES VRIEZE, DAVID M. GROVE,

Anorganisch Chemisch Laboratorium, J.H. van 't Hoff Instituut, University of Amsterdam, Nieuwe Achtergracht 166, 1018 WV Amsterdam (The Netherlands)

ENNO A. KLOP, ANTHONY L. SPEK *,

Laboratorium voor Struktuurchemie, University of Utrecht, Padualaan 8, 3584 CH Utrecht (The Netherlands)

and ALFRED SCHMIDPETER

Institut für Anorganische Chemie der Universität München, Meiserstrasse 1, D-8000 München 2 (B.R.D.)

(Received June 13th, 1983)

Summary

The azaphospholes $\overline{P{=}NN(Me)C(Me){=}N}$ (L_N) and $\overline{P{=}C(H)C(Me){=}NN(Me)}$ (L_C) have been used to synthesize the air-sensitive Pt^0 complexes $[Pt(PPh_3)_2L_2]$ and $[Pt(PPh_3)_3L]$ ($L = L_N$, L_C), which are stable towards dissociation in solution at $-40°C$. One representative $[Pt(PPh_3)_3L_N]$ (I) has been the subject of a single-crystal X-ray diffraction study. I is monoclinic, space group $P2_1/c$, with a 15.680(5), b 13.679(6), c 27.82(2) Å, β 113.86(4)°; $Z = 4$; $R = 0.071$ for 5492 observed reflections. The flat azaphosphole ligand is σ-P bonded to the metal centre (Pt–P 2.227(4) Å) which completes its pseudo-tetrahedral coordination sphere with the three PPh_3 groups ($Pt–P_{(av)}$ 2.337 Å). ^1H and ^{31}P NMR data for the new complexes are discussed.

Introduction

Recently there has been much interest in heteroolefinic compounds containing two-coordinate trivalent phosphorus doubly bonded to carbon or nitrogen, λ^3-phosphaalkenes -P=C< and λ^3-phosphazenes -P=N-, respectively [1]. Both acyclic and

* To whom correspondence should be addressed.

0022-328X/83/$03.00

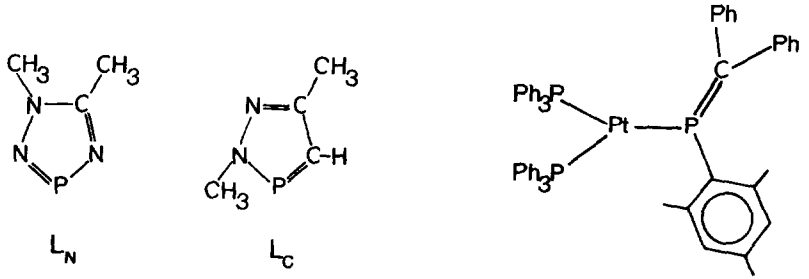

Fig. 1. 1,5-Dimethyl-1,2,4,3-triazaphosphole (L_N) and 2,5-dimethyl-1,2,3-diazaphosphole (L_C).

Fig. 2. Schematic structure of $[Pt(PPh_3)_2MesP{=}CPh_2]$.

cyclic species have been synthesized. The electron distribution in these compounds can be studied by investigating the availability of the *n*-electron pairs on phosphorus and nitrogen as well as of the π-electrons of the P=C or P=N bond for metal coordination.

In the azaphospholes (such as L_N and L_C, see Fig. 1) the phosphazene or phosphaethene group has become part of an aromatic heterocyclic system. Towards zerovalent Cr, Mo, W, Fe and Mn carbonyl fragments they coordinate via the phosphorus lone pair [2,3]. Structural and spectroscopic results indicate a P-donor ability in these complexes similar to that of triphenylphosphite (1,2,3-diazaphospholes) and triphenylphosphine (1,2,4,3-triazaphospholes). Other studies using Au^{III} centres [4], however, show the P-donor strength to be comparable to that of the pyridinic nitrogen, since coordination in $AuMe_2ClL$ (L = di- and triazaphospholes) switches from P to N depending upon the substituents and their position. Unfortunately the complexes $Au^{I}ClL$ were not amenable to spectroscopic studies, preventing a comparison of the ligands L in coordination with different oxidation states of the same metal.

To help elucidate these and other aspects of azaphosphole chemistry we are currently extending studies of the ligands 1,5-dimethyl-1,2,4,3-triazaphosphole (L_N) and 2,5-dimethyl-1,2,3-diazaphosphole (L_C) (Fig. 1) with Pt^0 and Pt^{II} as the metal coordination centres.

For example, in the case of Pt^0 one could expect not only σ-P coordination but also η^2-P=N(L_N) or η^2-P=C(L_C) coordination of the ligands. Such an ambivalent coordination behaviour was observed by us for a phosphaalkene in the complex $[Pt(PPh_3)_2MesP{=}CPh_2]$ [5a]; the solid state structure (Fig. 2) shows σ-P coordination, whereas in solution η^2-P=C bonding is clearly present [5].

In this paper we describe the reactions of L_N and L_C with $[Pt(PPh_3)_3]$ and $[Pt(PPh_3)_2C_2H_4]$ as the Pt^0 substrates, and the crystal and molecular structure of $[Pt(PPh_3)_3L_N]$. A future paper will be concerned with the coordination of L_N and L_C to Pt^{II} and Pd^{II}.

Experimental

All preparations were carried out under oxygen-free dry nitrogen. The solvents were carefully dried and distilled before use. The complexes $[Pt(PPh_3)_3]$ and

$[Pt(PPh_3)_2C_2H_4]$ [6] and the azaphosphole ligands [7,8] were prepared by published methods. The ^{31}P NMR spectra were recorded on Bruker WP 80 (32.4 MHz) and Varian XL-100 (40.5 MHz) spectrometers. The ^1H NMR spectra were recorded on a Bruker WM 250 spectrometer. Elemental analyses were carried out by the Elemental Analytical section of the Institute for Applied Chemistry TNO (Utrecht, The Netherlands).

Preparation of $[Pt(PPh_3)_3L_N]$

To a solution of L_N (1.27 mmol, 0.147 g) in 5 ml of toluene was added $[Pt(PPh_3)_3]$ (1.15 mmol, 1.13 g). The dark red solution was stirred at room temperature and within 30 min a yellow product began to separate. After 2 h 15 ml of pentane was added to the mixture and the pale yellow solid was filtered off, washed three times with 5 ml of pentane, and dried in vacuo for 2 h. Yield 92%. Recrystallization from warm toluene gave yellow crystals of the toluene solvate $[Pt(PPh_3)_3L_N]\cdot C_7H_8$.

Analyses: Found: C, 64.13; H, 5.00; N, 3.52; P, 10.07. $C_{64}H_{59}N_3P_4Pt$ calcd.: C, 64.58; H, 5.08; N, 3.53; P, 10.41%.

Preparation of $[Pt(PPh_3)L_C]$

To a solution of L_C (0.90 mmol, 0.103 g) in 5 ml of toluene was added $[Pt(PPh_3)_3]$ (0.82 mmol, 0.80 g). The dark red solution was stirred at room temperature, and after about 20 min, a yellow precipitate started to separate. After 2 h 15 ml of pentane was added, and the pale yellow solid was filtered off, washed 3 times with 5 ml of pentane, and dried in vacuo for 2 h. Yield 90%.

Analyses: Found: C, 63.40; H, 4.89; N, 2.52; P, 11.05. $C_{58}H_{52}N_2P_4Pt$ calcd.: C, 63.56; H, 4.76; N, 2.56; P, 11.30%.

Preparation of $[Pt(PPh_3)_2(L_N)_2]$

A solution of L_N (2.26 mmol 0.260 g) in 2 ml of toluene was added to $[Pt(PPh_3)_2C_2H_4]$ (0.40 mmol, 0.300 g) and the yellow suspension was stirred for 3 h at room temperature. After addition of 20 ml of pentane the pale yellow solid was filtered off, washed 4 times with 5 ml of pentane, and dried in vacuo for 1 h. Yield 74%.

Analyses: Found: C, 52.89; H, 4.87; N, 9.03; P, 12.48. $C_{42}H_{42}P_4N_6Pt$ calcd.: C, 53.11; H, 4.45; N, 8.85; P, 13.04%.

Preparation of $[Pt(PPh_3)_2(L_C)_2]$

A solution of L_C (1.58 mmol, 0.180 g) in 2 ml of toluene was added to $[Pt(PPh_3)_2C_2H_4]$ (0.31 mmol, 0.230 g). The brown-yellow solution was stirred at room temperature and after 1 h a further 1.58 mmol L_C was added, whereupon the solution became lighter in colour and finally, after 30 min, yellow. After a further 0.5 h the solution was cooled to $-20°C$ and the complex was precipitated by addition of 20 ml of pentane followed by cooling for 3 h at $-80°C$. The pale yellow product was filtered off at low temperature, washed twice with 5 ml of cold pentane, and dried in vacuo for 1 h. Yield 91%.

Analyses: Found: C, 55.22; H, 4.62; N, 6.49; P, 12.68. $C_{44}H_{44}N_4P_4Pt$ calcd.: C, 55.76; H, 4.68; N, 5.91; P, 13.07%.

X-Ray crystal structure determination of $C_{57}H_{51}N_3P_4Pt \cdot C_7H_8$

Data collection and reduction: Yellow crystals of the title complex were grown from toluene solution at room temperature and a suitable specimen was mounted in a Lindemann capillary under N_2 atmosphere.

Preliminary Weissenberg film data indicated that the crystal was monoclinic, space group $P2_1/c$. The crystal was transferred to an ENRAF NONIUS CAD 4F diffractometer for data collection. The setting angles of 16 carefully centred reflections were used in a least-squares calculation which led to the cell constants (Table 1). 20405 intensities up to $\theta = 25°$ were collected in the $w/2\theta$ scan mode using Zr-filtered Mo-K_α radiation. A decay of 10% was observed during data collection as monitored by the standard reflection (8 3 4). After merging equivalent reflections (merging index, 8%) a set of 9600 reflections was obtained of which 5492 with $I > 2.5\sigma(I)$ were used in the caleulations. Data were corrected for Lorentz and polarisation effects but not for absorption. The structure was solved by standard Patterson and Fourier methods and refined by anisotropic blocked full-matrix least-squares procedures with the programme ILIAS [9]. A difference Fourier map indicated that the crystal structure contained additional disordered toluene molecules of crystallization. Refinement was continued with a disorder model for toluene. Hydrogen atoms were included at calculated positions and refined in the riding mode on the parameters of their neighbouring atom, except for the methyl-hydrogen atoms which were refined as a rigid group.

Assignment of N(3) and C(55) was a problem, since these atoms could not be distinguished easily, neither from the chemical connectivity nor from peak heights in a difference map. On examining bond length information from the Cambridge Crystallographic Database it was found that N–N distances tend to be longer than N–C distances in triazole systems. The assignment of the PNNCN ring atoms, as shown in Fig. 3, is therefore based on the assumption that the distances of 1.31 and 1.39 Å are more likely to correspond to a C ··· N and a N ··· N bond, respectively than vice versa. The resulting model seems to fit reasonably, although the presence of the alternative form with N(3) and C(55) interchanged cannot be excluded. This

(Continued on p. 381)

TABLE 1

CRYSTALLOGRAPHIC DATA

Formula	$C_{57}H_{51}N_3P_4Pt \cdot C_7H_8$
MW	1189.2
Spacegroup	$P2_1/c$
Z	4
a (Å)	15.680(5)
b (Å)	13.679(6)
c (Å)	27.82(2)
β (deg.)	113.86(4)
V (Å^3)	5457(5)
D(calc) (g cm^{-3})	1.448
F(000)	2408
μ(Mo-K_α) (cm^{-1})	28.68
N	5492
R	0.071
R_w	0.066

TABLE 2

FRACTIONAL ATOMIC COORDINATES

Atom	x/a	y/b	z/c
Pt(1)	0.22222(4)	0.25963(3)	0.42600(2)
P(1)	0.2287(2)	0.4222(2)	0.4526(1)
P(2)	0.1742(2)	0.2529(3)	0.3352(1)
P(3)	0.1302(2)	0.1589(3)	0.4545(1)
P(4)	0.3682(3)	0.2042(3)	0.4611(2)
N(1)	0.4532(8)	0.218(1)	0.4421(5)
N(2)	0.4271(9)	0.1392(9)	0.5139(5)
N(3)	0.5159(9)	0.130(1)	0.5152(5)
C(1)	0.297(1)	0.5092(9)	0.4324(5)
C(2)	0.389(1)	0.481(1)	0.4414(6)
C(3)	0.448(1)	0.550(1)	0.4311(6)
C(4)	0.416(1)	0.639(1)	0.4114(6)
C(5)	0.326(1)	0.665(1)	0.4033(6)
C(6)	0.2684(9)	0.603(1)	0.4141(5)
C(7)	0.2836(9)	0.449(1)	0.5245(5)
C(8)	0.300(1)	0.372(1)	0.5580(5)
C(9)	0.340(1)	0.388(1)	0.6126(6)
C(10)	0.366(1)	0.479(1)	0.6318(6)
C(11)	0.348(1)	0.557(1)	0.5979(6)
C(12)	0.307(1)	0.540(1)	0.5442(5)
C(13)	0.1177(9)	0.4886(8)	0.4297(5)
C(14)	0.0852(9)	0.534(1)	0.4641(5)
C(15)	−0.002(1)	0.576(1)	0.4444(6)
C(16)	−0.057(1)	0.577(1)	0.3911(6)
C(17)	−0.024(1)	0.534(1)	0.3574(5)
C(18)	0.0628(9)	0.4903(9)	0.3767(5)
C(19)	0.195(1)	0.3629(9)	0.3037(5)
C(20)	0.287(1)	0.396(1)	0.3213(6)
C(21)	0.308(1)	0.473(1)	0.2962(6)
C(22)	0.242(1)	0.517(1)	0.2537(6)
C(23)	0.150(1)	0.486(1)	0.2349(6)
C(24)	0.127(1)	0.409(1)	0.2599(5)
C(25)	0.2266(9)	0.163(1)	0.3061(5)
C(26)	0.254(1)	0.071(1)	0.3314(6)
C(27)	0.279(1)	−0.004(1)	0.3061(8)
C(28)	0.284(1)	0.013(1)	0.2584(8)
C(29)	0.267(1)	0.101(1)	0.2374(6)
C(30)	0.234(1)	0.175(1)	0.2586(6)
C(31)	0.0493(8)	0.2351(9)	0.2950(4)
C(32)	0.012(1)	0.189(1)	0.2468(6)
C(33)	−0.082(1)	0.185(1)	0.2167(6)
C(34)	−0.144(1)	0.229(1)	0.2342(6)
C(35)	−0.107(1)	0.277(1)	0.2834(6)
C(36)	−0.0121(9)	0.276(1)	0.3133(5)
C(37)	0.166(1)	0.1477(9)	0.5266(5)
C(38)	0.106(1)	0.166(1)	0.5515(5)
C(39)	0.139(1)	0.160(1)	0.6052(6)
C(40)	0.230(1)	0.136(1)	0.6345(6)
C(41)	0.291(1)	0.116(1)	0.6116(6)
C(42)	0.2572(9)	0.124(1)	0.5566(5)
C(43)	0.005(1)	0.185(1)	0.4319(5)
C(44)	−0.064(1)	0.113(1)	0.4139(5)
C(45)	−0.157(1)	0.135(1)	0.3958(6)

TABLE 2 (continued)

Atom	x/a	y/b	z/c
C(46)	−0.184(1)	0.232(1)	0.3963(6)
C(47)	−0.117(1)	0.305(1)	0.4143(6)
C(48)	−0.022(1)	0.281(1)	0.4322(5)
C(49)	0.1263(9)	0.0273(9)	0.4377(5)
C(50)	0.104(1)	0.005(1)	0.3848(6)
C(51)	0.095(1)	−0.090(1)	0.3676(6)
C(52)	0.110(1)	−0.164(1)	0.4029(6)
C(53)	0.133(1)	−0.145(1)	0.4558(7)
C(54)	0.1396(9)	−0.048(1)	0.4721(6)
C(55)	0.528(1)	0.176(1)	0.4770(7)
C(56)	0.619(1)	0.171(2)	0.4734(9)
C(57)	0.587(1)	0.078(1)	0.5585(7)
C(58)	0.519(1)	0.187(1)	0.2989(8)
C(59)	0.481(1)	0.282(1)	0.2908(8)
C(60)	0.489(1)	0.341(1)	0.2522(8)
C(61)	0.535(1)	0.307(1)	0.2216(8)
C(62)	0.572(1)	0.213(1)	0.2298(8)
C(63)	0.564(1)	0.153(1)	0.2684(8)
C(64)	0.524(2)	0.107(2)	0.336(1)
C(65)	1.535(2)	0.252(2)	0.241(1)
C(66)	1.559(2)	0.153(2)	0.249(1)
C(67)	1.547(2)	0.102(2)	0.290(1)
C(68)	1.511(2)	0.149(2)	0.322(1)
C(69)	1.487(2)	0.248(2)	0.313(1)
C(70)	1.498(2)	0.299(2)	0.273(1)
C(71)	1.555(3)	0.287(3)	0.196(2)
H(2)	0.415(1)	0.409(1)	0.4560(6)
H(3)	0.519(1)	0.530(1)	0.4391(6)
H(4)	0.460(1)	0.689(1)	0.4019(6)
H(5)	0.301(1)	0.737(1)	0.3883(6)
H(6)	0.1991(9)	0.628(1)	0.4079(5)
H(8)	0.282(1)	0.299(1)	0.5427(5)
H(9)	0.350(1)	0.328(1)	0.6392(6)
H(10)	0.400(1)	0.490(1)	0.6737(6)
H(11)	0.367(1)	0.630(1)	0.6129(6)
H(12)	0.292(1)	0.601(1)	0.5175(5)
H(14)	0.1283(9)	0.536(1)	0.5058(5)
H(15)	−0.028(1)	0.609(1)	0.4711(6)
H(16)	−0.125(1)	0.611(1)	0.3760(6)
H(17)	−0.065(1)	0.534(1)	0.3155(5)
H(18)	0.0880(9)	0.4568(9)	0.3498(5)
H(20)	0.342(1)	0.360(1)	0.3542(6)
H(21)	0.379(1)	0.500(1)	0.3107(6)
H(22)	0.260(1)	0.576(1)	0.2345(6)
H(23)	0.097(1)	0.521(1)	0.2012(6)
H(24)	0.056(1)	0.384(1)	0.2454(5)
H(26)	0.255(1)	0.062(1)	0.3702(6)
H(27)	0.294(1)	−0.076(1)	0.3238(8)
H(28)	0.302(1)	−0.045(1)	0.2378(8)
H(29)	0.280(1)	0.117(1)	0.2026(6)
H(30)	0.214(1)	0.244(1)	0.2381(6)
H(32)	0.059(1)	0.155(1)	0.2322(6)
H(33)	−0.108(1)	0.147(1)	0.1795(6)
H(34)	−0.218(1)	0.227(1)	0.2112(6)

TABLE 2 (continued)

Atom	x/a	y/b	z/c
H(35)	−0.153(1)	0.316(1)	0.2973(6)
H(36)	0.0145(9)	0.307(1)	0.3525(5)
H(38)	0.035(1)	0.187(1)	0.5285(5)
H(39)	0.093(1)	0.173(1)	0.6244(6)
H(40)	0.254(1)	0.132(1)	0.6767(6)
H(41)	0.362(1)	0.096(1)	0.6350(6)
H(42)	0.3039(9)	0.110(1)	0.5375(5)
H(44)	−0.043(1)	0.037(1)	0.4144(5)
H(45)	−0.209(1)	0.078(1)	0.3808(6)
H(46)	−0.257(1)	0.250(1)	0.3827(6)
H(47)	−0.138(1)	0.380(1)	0.4148(6)
H(48)	0.031(1)	0.338(1)	0.4460(5)
H(50)	0.092(1)	0.064(1)	0.3570(6)
H(51)	0.077(1)	−0.106(1)	0.3266(6)
H(52)	0.104(1)	−0.239(1)	0.3897(6)
H(53)	0.145(1)	−0.203(1)	0.4837(7)
H(54)	0.1559(9)	−0.032(1)	0.5129(6)
H(59)	0.446(1)	0.308(1)	0.3145(8)
H(60)	0.460(1)	0.414(1)	0.2458(8)
H(61)	0.541(1)	0.353(1)	0.1917(8)
H(62)	0.607(1)	0.186(1)	0.2061(8)
H(63)	0.593(1)	0.080(1)	0.2747(8)
H(66)	1.587(2)	0.116(2)	0.225(1)
H(67)	1.566(2)	0.026(2)	0.296(1)
H(68)	1.502(2)	0.110(2)	0.353(1)
H(69)	1.459(2)	0.285(2)	0.338(1)
H(70)	1.479(2)	0.376(2)	0.267(1)
H(561)	0.617(1)	0.213(2)	0.4400(9)
H(562)	0.636(1)	0.096(2)	0.4688(9)
H(563)	0.672(1)	0.201(2)	0.5089(9)
H(571)	0.652(1)	0.077(1)	0.5531(7)
H(572)	0.565(1)	0.003(1)	0.5597(7)
H(573)	0.598(1)	0.114(1)	0.5950(7)
H(641)	0.490(2)	0.130(2)	0.360(1)
H(642)	0.596(2)	0.091(2)	0.360(1)
H(643)	0.490(2)	0.043(2)	0.314(1)
H(711)	1.539(3)	0.363(3)	0.187(2)
H(712)	1.516(3)	0.242(3)	0.162(2)
H(713)	1.629(3)	0.275(3)	0.207(2)

problem was not pursued further in view of the quality of the dataset. The final model with 620 parameters converged to R and R_w values of 0.066 and 0.071, respectively.

The weighting scheme employed was: weight $= 2.1459/(\sigma^2(F) + 0.001\ F^2)$. A final difference Fourier map revealed nine peaks of density ranging from 1.1 to 3.1 eÅ^{-3} which are ascribed to absorption and decay effects. Scattering factors of Cromer and Mann [10] were used. Anomalous dispersion terms were taken from Cromer and Liberman [11].

The atomic coordinates are listed in Table 2. Complete lists of the structural parameters and temperature factors are available from one of the authors (A.L.S.).

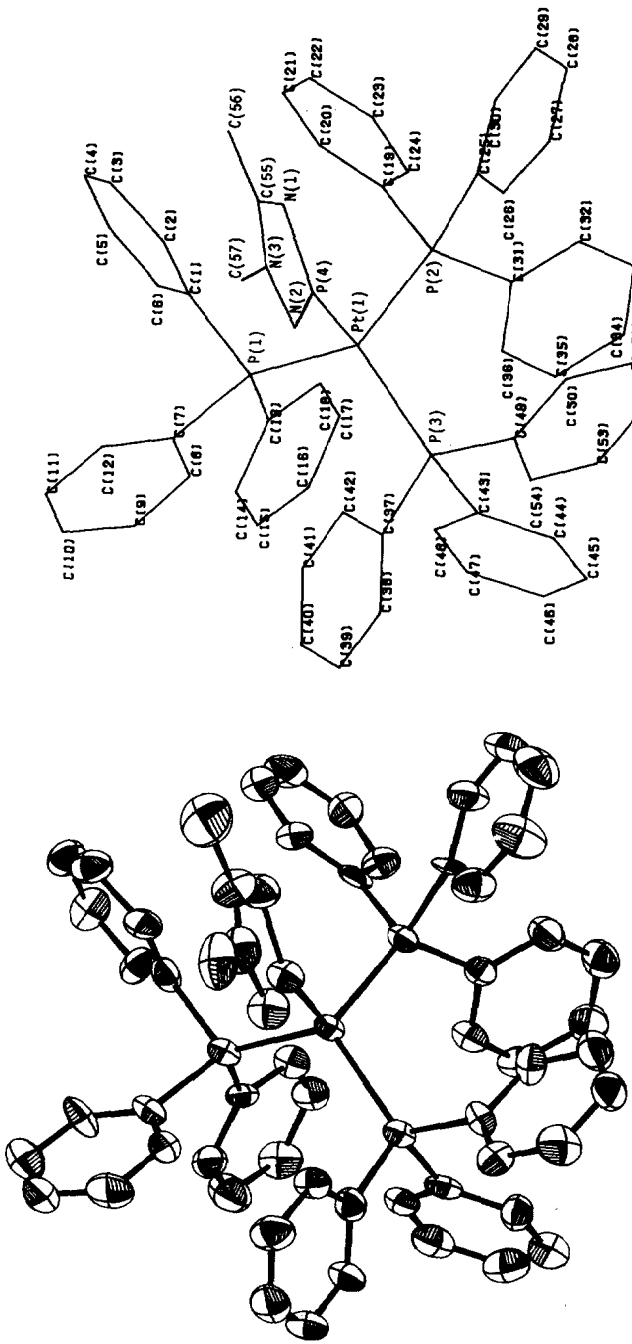

Fig. 3. ORTEP view of $C_{57}H_{51}N_3P_4Pt$ along with adopted numbering scheme.

Results

In contrast to the results of Scherer et al. [12], who observed that [Pt(RR'N–P=NR'')$_3$] was formed in the reaction of RR'N–P=N–R'' with [Pt(COD)$_2$], we found that L (L = L_N, L_C) leads to decomposition products with this particular Pt^0 substrate. However, both L_N and L_C react with [Pt(PPh$_3$)$_3$] in a 1/1 ratio to afford the species [Pt(PPh$_3$)$_3$L] (eq. 1), which may be isolated as yellow crystalline solids in high yield. The complexes [Pt(PPh$_3$)$_2$L$_2$] have been synthesized similarly from the 4/1 reaction of L and [Pt(PPh$_3$)$_2$C$_2$H$_4$] (eq. 2).

$$[Pt(PPh_3)_3] + L \xrightarrow[RT]{\text{toluene,}} [Pt(PPh_3)_3L] \quad (1)$$

$$[Pt(PPh_3)_2C_2H_4] + 4L \xrightarrow[RT]{\text{toluene,}} [Pt(PPh_3)_2L_2] + 2L + C_2H_4 \quad (2)$$

In the latter reaction when two equivalents of azaphosphole are used a variety of as yet unidentified species (some presumably containing C_2H_4) are formed, together with [Pt(PPh$_3$)$_3$L]. Only when an excess of ligand is present does isolation of pure [Pt(PPh$_3$)$_2$L$_2$] become possible. Introduction of a third azaphosphole does not appear to take place under these conditions.

All these new compounds, whose stoichiometry has been established by elemental analyses and ^{1}H and ^{31}P NMR data (see Tables 3, 4), are air sensitive, and are readily soluble in toluene or dichloromethane but practically insoluble in pentane or hexane. It should be emphasized that like most tetrahedral Pt^0 phosphine complexes, these new isolated species give temperature dependent ^{31}P NMR spectra, and limiting data were obtained at −40°C in toluene-d_8 or dichloromethane-d_2.

A typical illustrative spectrum, that of [Pt(PPh$_3$)$_2$(L$_C$)$_2$], is presented in Fig. 4. As with all the other new azaphosphole species, the multiplicity of the ^{31}P NMR signals suggests a tetrahedral metal coordination sphere of four phosphine donor ligands, with large ^1J(Pt,P) values which may be considered characteristic for zerovalent Pt compounds. However, unlike many [Pt(PR$_3$)$_4$] systems the spectra so obtained essentially contain only the appropriate four coordinate Pt^0 species, with no evidence for three coordinate species. On consideration of the possible equilibria

$$[Pt(PPh_3)_4] \rightleftarrows [Pt(PPh_3)_3] + PPh_3$$

$$\text{and } [Pt(PPh_3)_3L] \rightleftarrows [Pt(PPh_3)_3] + L$$

TABLE 3

^{1}H NMR DATA FOR [Pt(PPh$_3$)$_n$L$_{(4-n)}$] (n = 2, 3) [a]

Compound	δ(P=CH)	^2J(P,CH)	δ(NMe)	^nJ(P,NMe) [b]	δ(CMe)	^4J(P,CMe)
L_N [f]			4.07	1.4	2.65	0.7
Pt(PPh$_3$)$_3$L$_N$ [c]			3.75	<1	2.42	<1
Pt(PPh$_3$)$_2$(L$_N$)$_2$ [c]			3.80	<1	2.46	<1
L_C [f]	7.25	43.7	3.66	7.6	2.33	1.3
Pt(PPh$_3$)$_3$L$_C$ [c]	5.32 [d]	42.9	2.93	8.5	2.12	<1
Pt(PPh$_3$)$_2$(L$_C$)$_2$ [c]	6.07 [e]	42.9	3.46	7.7	2.17	<1

[a] The spectra were recorded at −40°C in CD_2Cl_2, δ(ppm) relative to TMS, coupling constants in Hz. [b] ^4J(PNNMe) (L_N) or ^3J(PNMe) (L_C) [c] The PPh_3 signals were found in the range 6.75–7.75 ppm. [d] ^3J(PtPCH) 47 Hz. [e] ^3J(PtPCH) was not observed. [f] Data from ref. 2.

TABLE 4

^{31}P NMR DATA FOR $[Pt(PPh_3)_nL_{(4-n)}]$ ($n = 2,3,4$) AND $[Pt(PPh_3)_3CO]$ [a]

Complex	PPh_3		P′ (L_N or L_C)		$^2J(P,P')$
	$\delta(P)$	$^1J(Pt-P)$	$\delta(P')$	$^1J(Pt-P')$	
$Pt(PPh_3)_3L_N$ [b]	14.2(d)	4068	234.4(q)	3580	55
$Pt(PPh_3)_3L_C$ [b]	12.4(d)	4051	204.3(q)	3475	57
$Pt(PPh_3)_2(L_N)_2$ [b]	18.8(t)	4138	237.8(t)	4377	54
$Pt(PPh_3)_2(L_N)_2$ [c]	13.0(t)	4094	231.0(t)	4428	53
$Pt(PPh_3)_2(L_C)_2$ [b]	12.2(t)	4097	195.9(t)	3887	57
$Pt(PPh_3)_2(L_C)_2$ [c]	12.6(t)	4163	197.9(t)	3942	57
$Pt(PPh_3)_4$ [b]	9.1(s)	3814			
$Pt(PPh_3)_3CO$ [b]	13.1(s)	3593			

[a] The spectra were recorded at −40°C, (ppm) relative to external 85% H_3PO_4, downfield shifts being positive, coupling constants in Hz. [b] In toluene-d_8. [c] In CD_2Cl_2.

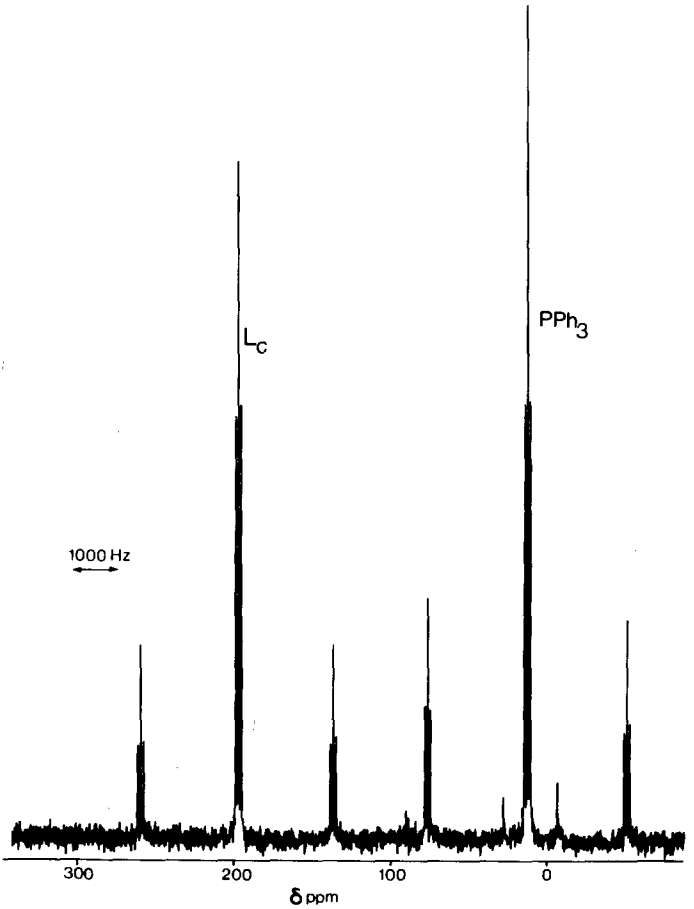

Fig. 4. 32.4 MHz ^{31}P NMR spectrum of $[Pt(PPh_3)_2(L_c)_2]$ in CD_2Cl_2 at −40°C.

this latter observation implies that the azaphosphole is more strongly bound than PPh_3. The same conclusion may also be drawn for the coordination of a second azaphosphole, since ^{31}P NMR measurements of a 1/1 mixture of $[Pt(PPh_3)_3L]$ and azaphosphole ($-40°C$, CD_2Cl_2) shows that the equilibrium.

$$Pt(PPh_3)_3L + L \rightleftharpoons [Pt(PPh_3)_2L_2] + PPh_3$$

lies predominantly over to the right hand side.

To help understand this behaviour, and to ensure correct characterization of these new azaphosphole complexes in the solid state, particularly with regard to the ligand coordination mode, we undertook a crystallographic study of a representative member, $[Pt(PPh_3)_3L_N]$.

Description of the molecular geometry of $[Pt(PPh_3)_3L_N] \cdot C_7H_8$

The crystal structure of the title compound involves the packing of 4 discrete molecules of the complex and 4 disordered toluene molecules in the unit cell. Figure 3 presents an ORTEP view of the complex and sets out the numbering scheme. The disorder model used for toluene is shown in Fig. 5.

Some selected bond lengths, bond angles and non-bonding contact distances and angles are presented in Table 5.

The central Pt atom, which is coordinated to four P-donor ligands, has a slightly deformed tetrahedral configuration with Pt–PPh_3 distances (2.327(3), 2.333(3) and 2.352(4) Å) significantly longer than the Pt–P (azaphosphole) distance (2.227(4) Å).

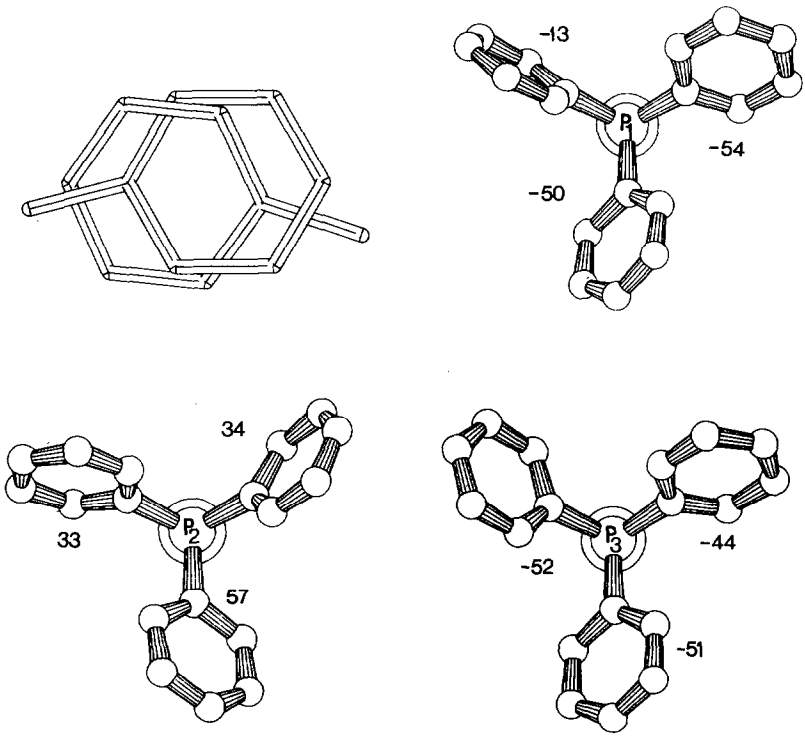

Fig. 5. Toluene disorder model; PLUTO drawing of PPh_3 ligands with the torsion angles Pt–P–C(a)–C(b),C(b) closest to Pt.

TABLE 5

SELECTED GEOMETRICAL DATA

Bond lengths (Å)

Pt(1)–P(1)	2.333(3)	P(2)–C(19)	1.84(1)	P(4)–N(2)	1.64(1)
Pt(1)–P(2)	2.327(3)	P(2)–C(25)	1.84(1)	N(1)–C(55)	1.31(2)
Pt(1)–P(3)	2.352(4)	P(2)–C(31)	1.84(1)	N(2)–N(3)	1.39(2)
Pt(1)–P(4)	2.227(4)	P(3)–C(37)	1.86(2)	N(3)–C(55)	1.32(2)
P(1)–C(1)	1.83(1)	P(3)–C(43)	1.84(1)	N(3)–C(57)	1.46(2)
P(1)–C(7)	1.87(2)	P(3)–C(49)	1.85(1)	C(55)–C(56)	1.48(3)
P(1)–C(13)	1.83(1)	P(4)–N(1)	1.63(1)		
$^{+}\langle$C–C$\rangle$ P(1)	1.380(5)	$\langle$C–C$\rangle$ P(2)	1.384(6)	$\langle$C–C$\rangle$ P(3)	1.383(5)

$^{+}\langle$C–C$\rangle$ P(i) is the average of C–C bond lengths for P(i)$(Ph)_3$

Bond angles (deg.)

P(1)–Pt(1)–P(2)	109.6(1)	Pt(1)–P(3)–C(37)	117.1(5)
P(1)–Pt(1)–P(3)	113.9(1)	Pt(1)–P(3)–C(43)	119.2(5)
P(1)–Pt(1)–P(4)	106.3(1)	Pt(1)–P(3)–C(49)	116.5(5)
P(2)–Pt(1)–P(3)	111.7(1)	C(37)–P(3)–C(43)	101.3(7)
P(2)–Pt(1)–P(4)	106.7(1)	C(37)–P(3)–C(49)	99.0(6)
P(3)–Pt(1)–P(4)	108.3(1)	C(43)–P(3)–C(49)	100.3(6)
Pt(1)–P(1)–C(1)	118.6(5)	Pt(1)–P(4)–N(1)	130.4(5)
Pt(1)–P(1)–C(7)	118.0(5)	Pt(1)–P(4)–N(2)	133.1(5)
Pt(1)–P(1)–C(13)	116.6(4)	N(1)–P(4)–N(2)	96.5(7)
C(1)–P(1)–C(7)	97.3(7)	P(4)–N(1)–C(55)	108.(1)
C(1)–P(1)–C(13)	99.2(6)	P(4)–N(2)–N(3)	106.(1)
C(7)–P(1)–C(13)	103.6(6)	N(2)–N(3)–C(55)	114.(1)
Pt(1)–P(2)–C(19)	116.3(5)	N(2)–N(3)–C(57)	120.(1)
Pt(1)–P(2)–C(25)	120.0(5)	C(55)–N(3)–C(57)	126.(1)
Pt(1)–P(2)–C(31)	117.7(4)	N(1)–C(55)–N(3)	115.(1)
C(19)–P(2)–C(25)	97.9(6)	N(1)–C(55)–C(56)	125.(2)
C(19)–P(2)–C(31)	99.8(6)	N(3)–C(55)–C(56)	119.(2)
C(25)–P(2)–C(31)	101.5(6)		

Nonbonding contact distances (Å) and angles (deg.)

N(1)–H(2)	2.74(2)	C(2)–H(2)–N(1)	152.4 (15)
N(1)–H(20)	3.06(2)	C(20)–H(20)–N(1)	164.2 (13)
N(2)–H(42)	2.31(2)	C(42)–H(42)–N(2)	156.6 (13)

The angles between the Pt–PPh_3 bonds (ranging from 109.6(1) to 113.9(1)°) are somewhat larger than the ideal tetrahedral value, while those in which the Pt–triazaphosphole bond participates are somewhat smaller (ranging from 106.3(1) to 108.3(1)°).

The three PPh_3 ligands show no unusual features, with the carbon–carbon distances within the compound studied ranging from 1.32(3) to 1.42(2) Å; the average of the 54 independent values is 1.382(3) Å. The triphenylphosphine ligands have a propellor conformation, with the three phenyl rings twisted from the respective C–P–Pt planes in the same direction (Fig. 5). The shortest non-bonding

contact distance between an N atom of the triazaphosphole ligand and the triphenylphosphine ligands is 2.31(2) Å (Table 5).

Discussion

Although the organic chemistry of azaphospholes has been much studied, only a few types of complexes containing these ligands have been isolated [2,3,4]. There are many interesting aspects of such complexes, such as the influence of the metal oxidation state on the coordination mode(s) of these ambidentate ligands and the way this affects the further reactions of the azaphosphole unit.

In this work we have shown that, despite the availability of alternative bonding modes, the azaphospholes L_N and L_C show exclusively P coordination with zerovalent platinum substrates. The complexes $[Pt(PPh_3)_3L]$ and $[Pt(PPh_3)_2L_2]$ therefore, not unexpectedly, bear a resemblance to the isoelectronic d^{10} $[Pt(PR_3)_4]$ (R = aryl, alkyl) [13] complexes, and are characteristically air-sensitive in solution and the solid state. At room temperature, like the tetrakisphosphine complexes, the new Pt^0 azaphosphole species undergo ligand exchange processes on the NMR timescale. However, limiting ^{31}P NMR spectra (−40°C) show only the original species, with no evidence for either three coordinate species and free ligand(s) or mixtures of four coordinate $[Pt(PPh_3)_nL_{4-n}]$. Therefore it may be concluded that three coordinate $[Pt(PPh_3)_2L]$ must be intrinsically unstable with respect to the latter species. This is emphasized by the fact that reaction of $[Pt(PPh_3)_2(C_2H_4)]$ with L (one equivalent), the method most likely to produce $[Pt(PPh_3)_2L]$, only generates four coordinate Pt^0 species. In this respect it is clear that with soft Pt^0 the aromatic azaphospholes exhibit behaviour which differentiates them from other phosphorus donors such as tertiary phosphines or phosphaalkenes.

It was noted in the results that the nature of the ^{31}P NMR spectra, the synthetic method employed, and the possible equilibria to be expected with these Pt^0 species together suggest that L_N and L_C are stronger ligands than PPh_3. An approximate qualitative guide to the intrinsic electronic properties of these and other ligands capable of stabilizing four coordinate Pt^0 can be obtained by comparing appropriate ^{31}P NMR parameters (Table 4). For example, the trend in $^1J(Pt,PPh_3)$ in $[Pt(PPh_3)_3L']$ (L′ = CO, PPh_3, L_N, L_C) gives an order for overall electron donation to the metal of $L_N \approx L_C > PPh_3 > CO$. From this series it may be concluded that L_N and L_C have comparatively weak π-acceptor properties.

Comparison of $^1J(Pt,P)$ for the azaphospholes themselves reveals that in both $[Pt(PPh_3)_3L]$ and $[Pt(PPh_3)_2L_2]$ it is L_N which has the consistently higher one bond coupling to the metal than L_C. This is in agreement with the results obtained by other workers for $[W(CO)_5L']$ (L′ = phosphorus donor), which show that $^1J(W,P)$ increases with increasing substituent electronegativity [14]. It is also noteworthy that in these tungsten complexes the coupling constant for PPh_3 (280 Hz) [15] is a little larger than that for L_C (276 Hz) [2]; whereas in $[Pt(PPh_3)_3L']$ (L′ = PPh_3, L_C) the difference in $^1J(Pt,P)$ is comparatively much greater, the values being 3814 and 3475 Hz, respectively.

The crystallographic analysis of $[Pt(PPh_3)_3L_N]$ revealed, as was anticipated from the $^1J(Pt,P)$ and $\delta(P)$ values, that L_N is P-coordinated.

The structural features of this platinum complex and $[Pt(PPh_3)_3CO]$ show two particularly interesting aspects (See Table 6).

TABLE 6

COMPARISON OF METAL-CENTRED BOND ANGLES (°) AND BOND LENGTHS (Å) IN $[Pt(PPh_3)_3L_N]$ AND $[Pt(PPh_3)_3CO]$

	$[Pt(PPh_3)_3L_N]$	$[Pt(PPh_3)_3CO]$ [a]
Lengths		
Pt–P(Ph_3)	2.327(3)	2.333(8)
Pt–P(Ph_3)	2.333(3)	2.333(8)
Pt–P(Ph_3)	2.352(4)	2.352(8)
Pt–P(L_N)	2.227(4)	–
Angles [b]		
P–Pt–P	109.6(1)	109.6(2)
P–Pt–P	111.7(1)	110.9(3)
P–Pt–P	113.9(1)	113.7(3)

[a] Data from Ref. 16. [b] Between PPh_3 ligands only.

First, the angles defining the pseudotetrahedral geometry of the metal centres are closely comparable. This is presumably because both linear CO and flat L_N with limited steric bulk are unlikely to greatly affect the coordination sphere, so that the precise configuration is to a large extent determined by the interactions of the three triphenylphosphine ligands.

Second, the very similar Pt–P(sp^3) distances in the two complexes do not reflect the different electronic properties of L_N and CO though, not unexpectedly, these bond lengths are considerably larger than those in $[Pt(PPh_3)_3]$ (2.25–2.28 Å) [17]; this is a natural consequence of the presence of the electron pair which a good σ donor such as CO or L_N will add to the metal electron count.

As might be expected from consideration of the phosphorus hybridization, the Pt–P bond for the azaphosphole (2.227(4) Å, sp^2 P) is found to be much shorter than for the tertiary phosphines (~ 2.33–2.35 Å, sp^3 P). The same effect is also seen in the Pt–P(sp^2) distances of $[Pt^{II}Cl_2PEt_3MesP{=}CPh_2]$ [18] and $[Pt^0(PPh_3)_2MesP{=}CPh_2]$ [5] which are 2.199(2) and 2.218(3) Å, respectively. Upon coordination in $[Pt(PPh_3)_3L_N]$ the free azaphosphole ligand does not undergo any large structural changes, the N–P–N angle and the average interatomic ring distance being virtually identical in both situations (See Table 7). Furthermore, combined with other structural information, such as the coplanarity of this ring system and the Pt–P(L_N) bond, there is no evidence for a hybridization change of the sp^2 phosphorus centre.

All the data taken together provide a consistent picture of the azaphosphole ligands L_N and L_C acting towards Pt^0 as good σ-donors with low π-acceptor properties.

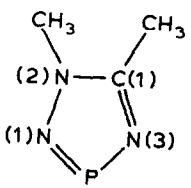

Fig. 6. L_N with the adopted numbering scheme for Table 7.

TABLE 7

COMPARATIVE BOND LENGTHS (Å) IN FREE AND COORDINATED L_N [a]

Bond	L_N	$[Pt(PPh_3)_3L_N]$
P–N(1)	1.638(4)	1.64(1)
P–N(3)	1.636(3)	1.63(1)
N(1)–N(2)	1.332(5)	1.39(2)
N(2)–C(1)	1.342(5)	1.32(2)
N(3)–C(1)	1.341(5)	1.31(2)
C(1)–C(2)	1.465(6)	1.48(3)
N(2)–C(3)	1.460(6)	1.46(2)

[a] Numbering is as shown in Fig. 6; free ligand distances are taken from ref. 19.

Acknowledgement

Thanks are due to Dr. A.J.M. Duisenberg for collecting the X-ray data and J.M. Ernsting for recording the NMR spectra.

This investigation was supported in part by the Netherlands Foundation for Chemical Research (SON) with financial aid from the Netherlands Organization for Pure Research (Z.W.O.) (A.L.S.).

References

1 Reviews: (a) E. Fluck, Top. Phosphorus Chem., 10 (1980) 194; (b) R. Appel, F. Knoll and I. Ruppert, Angew. Chem., 93 (1981) 771; Angew. Chem. Int. Ed. Engl., 20 (1981) 731.
2 J.H. Weinmaier, H. Tautz, A. Schmidpeter and S. Pohl, J. Organomet. Chem., 185 (1980) 53.
3 K. Issleib, H. Oehme, H. Schmidt and G.-R. Vollmer, ACS Symposium Series, 171 (1981) 403.
4 K.C. Dash, H. Schmidbaur and A. Schmidpeter, Inorg. Chim. Acta, 46 (1980) 167.
5 (a) Th.A. van der Knaap, F. Bickelhaupt, H. van der Poel, G. van Koten and C.H. Stam, J. Amer. Chem. Soc., 104 (1982) 1756; (b) Th.A. van der Knaap, J.G. Kraaijkamp, F. Bickelhaupt and G. van Koten, to be published.
6 R.R. Hartley, Organometal. Chem. Rev., A 6 (1970) 119.
7 A. Schmidpeter, J. Luber and H. Tautz, Angew. Chem., 89 (1977) 554; Angew. Chem. Int. Ed. Engl., 16 (1977) 546.
8 J.H. Weinmaier, G. Brunnhuber and A. Schmidpeter, Chem. Ber., 113 (1980) 2278.
9 ILIAS-A DG-Eclipse/S 230-minicomputer crystallographic program package derived from G. Sheldrick's SHELX-76.
10 D.T. Cromer and J.B. Mann, Acta Cryst. A24 (1968) 321.
11 D.T. Cromer and D. Liberman, J. Chem. Phys., 53 (1970) 1891.
12 O.J. Scherer, R. Konrad, C. Krüger and Y.H. Tsay, Chem. Ber., 115 (1982) 414.
13 B.E. Mann and A. Musco, J. Chem. Soc., Dalton Trans., (1980) 776 and references therein.
14 E.O. Fischer, L. Knaues, R.L. Keiter and J.G. Verkade, J. Organomet. Chem., 37 (1972) C7; H. Schumann and H.-J. Kroth, Z. Naturforsch. B, 32 (1977) 768.
15 S.O. Grim, P.R. McAllister and R.M. Singer, J. Chem. Soc. D., (1969) 38.
16 V.G. Albano, P.L. Bellon and M. Sansoni, Chem. Commun., (1969) 899; V.G. Albano, G.M. Basso Ricci and P.L. Bellon, Inorg. Chem., 8 (1969) 2109.
17 V. Albano, P.L. Bellon and V. Scatturin, Chem. Commun., (1966) 507.
18 H.W. Kroto, J.F. Nixon, M.J. Taylor, A.A. Frew and K.W. Muir, Polyhedron, 1 (1982) 89.
19 S. Pohl, Chem. Ber., 112 (1979) 3159.